Supporting Information for

Pseudocapacitive layered birnessite sodium manganese dioxide for high-rate non-aqueous sodium ion capacitors †

Yalong Jiang,[a] Shuangshuang Tan,[a] Qiulong Wei,*[b] Jun Dong,[a] Qidong Li,[a] Fangyu Xiong,[a] Jinzhi Sheng,[a] Qinyou An,[a] Liqiang Mai*[a]

[a]State Key Laboratory of Advanced Technology for Materials, Synthesis and Processing, International School of Materials Science and Engineering, Wuhan University of Technology, Wuhan 430070, China. *E-mail: mlq518@whut.edu.cn.

[b]Department of Materials Science and Engineering, University of California Los Angeles, Los Angeles, CA 90095-1595, USA. E-mail: *E-mail: qlwei@ucla.edu

Experiment

1. Synthesis and characterization of *b*-NMO/C, *b*-NMO and *b*-NMO/C-HT

The layered *b*-NMO/C was synthesized by a facile co-precipitation method under water bath.[30-32] A manganese nitrate aqueous solution (0.5 M, 30 mL) was prepared firstly. Then, carbon nanotubes (CNTs, 50 mg) and Ketjenblacks (KBs, 40 mg) were added to the obtained manganese nitrate solution with ultrasonic treatment for 30 min. A mixture solution of sodium hydroxide (1 M, 54 mL) and hydrogen peroxide (30 wt%, 10 mL) was added to the above suspension under vigorous stirring. Next, the suspension was aged in water bath for 24 h at 50 ^{o}C. The precipitant was collected after three times of filtration via centrifugation in DI water at 8000 rpm for 5 min. The final product was then obtained after drying in a vacuum oven at 60 °C overnight. The *b*-NMO was prepared through the same process of the *b*-NMO/C without the addition of carbon additives. The *b*-NMO/C-HT was synthesized by an additional heat-treatment of *b*-NMO/C at 400°C in argon for 4 h. The XRD patterns were recorded by a D8 Advance X-ray diffractometer with a Cu Kα radiation. The SEM images were collected with a JEOL-7100F microscope at an acceleration voltage of 20 kV. TEM, HRTEM images and energy dispersive X-ray spectra (EDS) elemental mappings were recorded by using a Titan G2 60-300. FT-IR spectra were obtained using a Nexus system. BET surface areas were measured using a Tristar II 3020 instrument by adsorption of nitrogen at 77 K. Inductively coupled plasma (ICP) test was performed on the PerkinElmer Optima 4300DV spectrometer. CHN elemental analyzer was involved in determining the carbon contents in the as-prepared samples.

The tested electrodes for *ex*-situ characterization were obtained by taking apart the coin cells in a glovebox filled with pure argon gas and washed with diethylene glycol dimethyl ether and alcohol and dispersed in alcohol with ultrasonic treatment.

2. Preparation of electrode and electrochemical tests

The electrochemical properties were characterized in 2016-type coin cells with sodium metal foil as the anode. The cathode electrodes of *b*-NMO/C and *b*-NMO/C-HT were composed of 85% active material, 10% Ketjenblacks (KBs) and 5% polyvinylidene fluoride (PVDF) with an appropriate amount of N-methyl-2-pyrrolidone (NMP) as solvent. As for cathode electrode of *b*-NMO, to control the same amount of carbon in the composite, 85% active material (92% *b*-NMO powder, 4.4% CNTs and 3.6% KBs was previously mixed by grinding), 10% KBs and 5% polyvinylidene fluoride (PVDF) were mixed with an appropriate amount of N-methyl-2-pyrrolidone (NMP) as well. The slurry was casted onto carbon coated aluminum foil and dried under a vacuum oven at 120 °C for 12 h. The mass loading of active material is 1–1.5 mg cm^{-2}. The specific capacity was calculated based on the amount of active materials. The graphite anode were prepared by mixing 92% active material and 8% CMC binder, and then coated on Al foil. The mass loading of active material is 2~3 mg cm^{-2}. For assemble the full *b*-NMO/C//Graphite sodium ion capacitor, the mass ratio of cathode: anode is adjusted to 1:1.6, while the cathode is presodiated previously. 1 M $NaPF_6$ in diethylene glycol dimethyl ether was used as the electrolyte. The cells were assembled in an argon-filled glove-box. The cyclic voltammetry, galvanostatic charge-discharge, and electrochemical impedance spectra

(ranging from 0.1 to 10^5 Hz) tests were carried out by a multichannel battery testing system (Bio–Logic VMP-300). All the measurements were carried out at room temperature.

3. Calculation of Brunauer-Emmett-Teller (BET) specific surface areas

The BET specific surface areas of *b*-NMO/C, *b*-NMO, carbon nanotubes (CNTs) and Ketjenblacks (KBs) are 26.0, 0.4, 200 and 1400 m^2 g^{-1}, respectively. Determined from CHN elemental analysis, the carbon contents of *b*-NMO/C is 8.09%. Firstly, the specific surface areas of carbon additives are denoted as C_{BET}, and the specific surface areas of *b*-NMO/C can be descripted as following Equation 1:

$$b-\mathrm{NMO/C}_{BET} = b-\mathrm{NMO}_{BET} * 91.91\% + \mathrm{C}_{BET} * 8.09\% \quad (1)$$

According to the calculation, the specific surface areas of carbon additives are about 316.8 m^2 g^{-1}. Thus, the enlarged surface of the *b*-NMO/C mainly comes for the existence of the carbon additives.

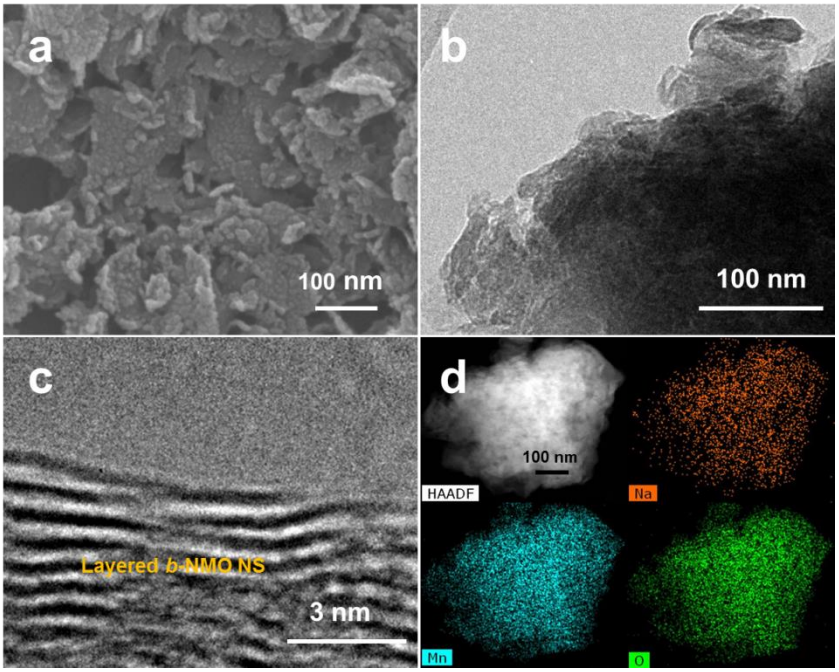

Figure S1. The SEM image (a), TEM image (b), HRTEM image (c) of the *b*-NMO. (d) The EDS element mappings of the *b*-NMO, showing the uniform distribution of Na, Mn and O.

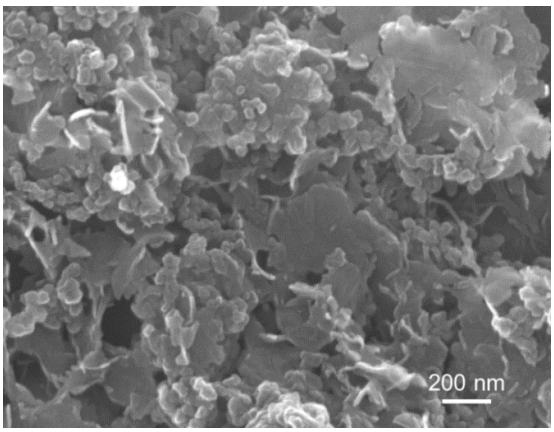

Figure S2. The SEM image of the *b*-NMO/C-HT.

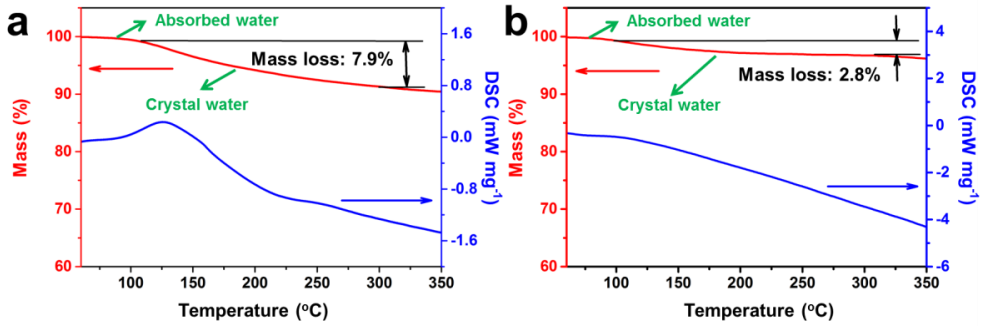

Figure S3. TG and DSC curves of the *b*-NMO (a) and *b*-NMO/C-HT (b). The mass loss of 7.9% and 2.8% comes from the crystal water loss in the range of 100 to 300 °C. Combining with the data of ICP (Table S1) and CHN (Table S2), the as-synthesized *b*-NMO and *b*-NMO/C-HT are identified as $Na_{0.77}MnO_2 \cdot 0.5H_2O$/C and $Na_{0.77}MnO_2 \cdot 0.18H_2O$/C.

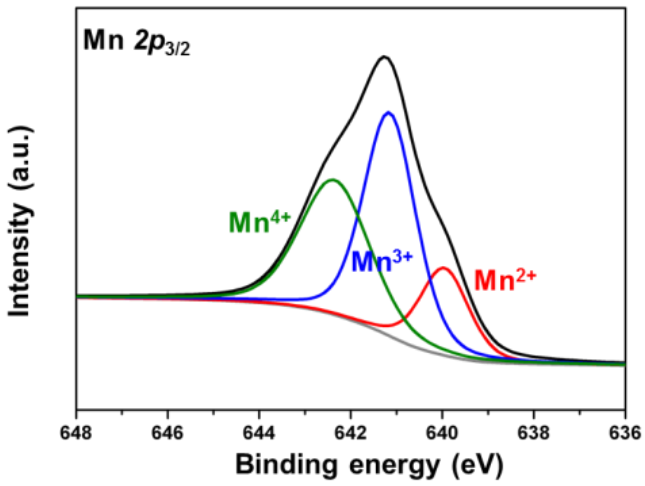

Figure S4. XPS spectra of Mn $2p_{3/2}$ core level of *b*-NMO/C.

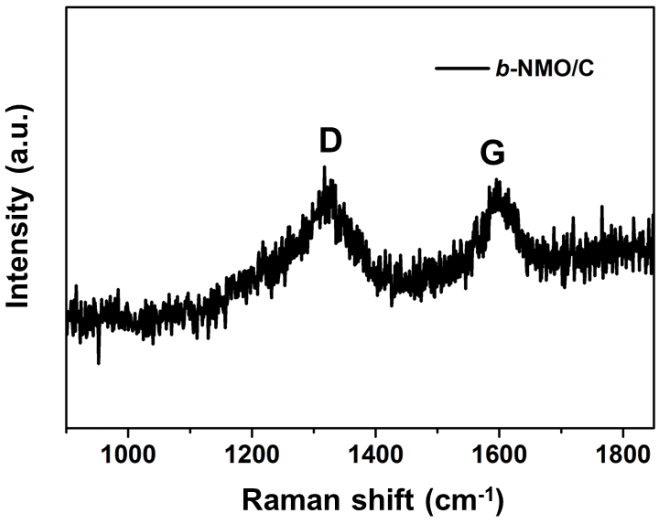

Figure S5. Raman spectrum of b-NMO/C.

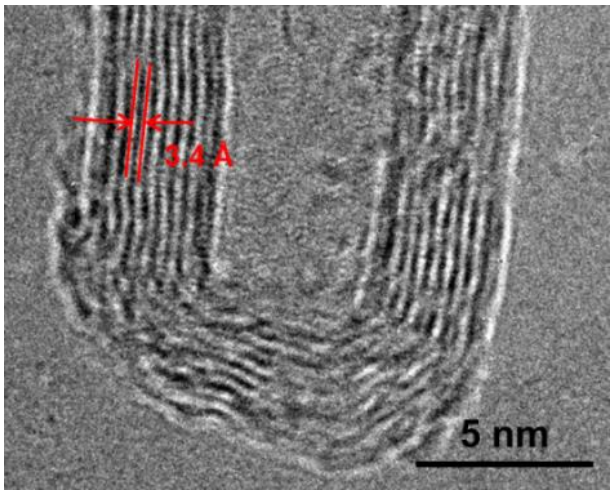

Figure S6. HRTEM image of CNTs.

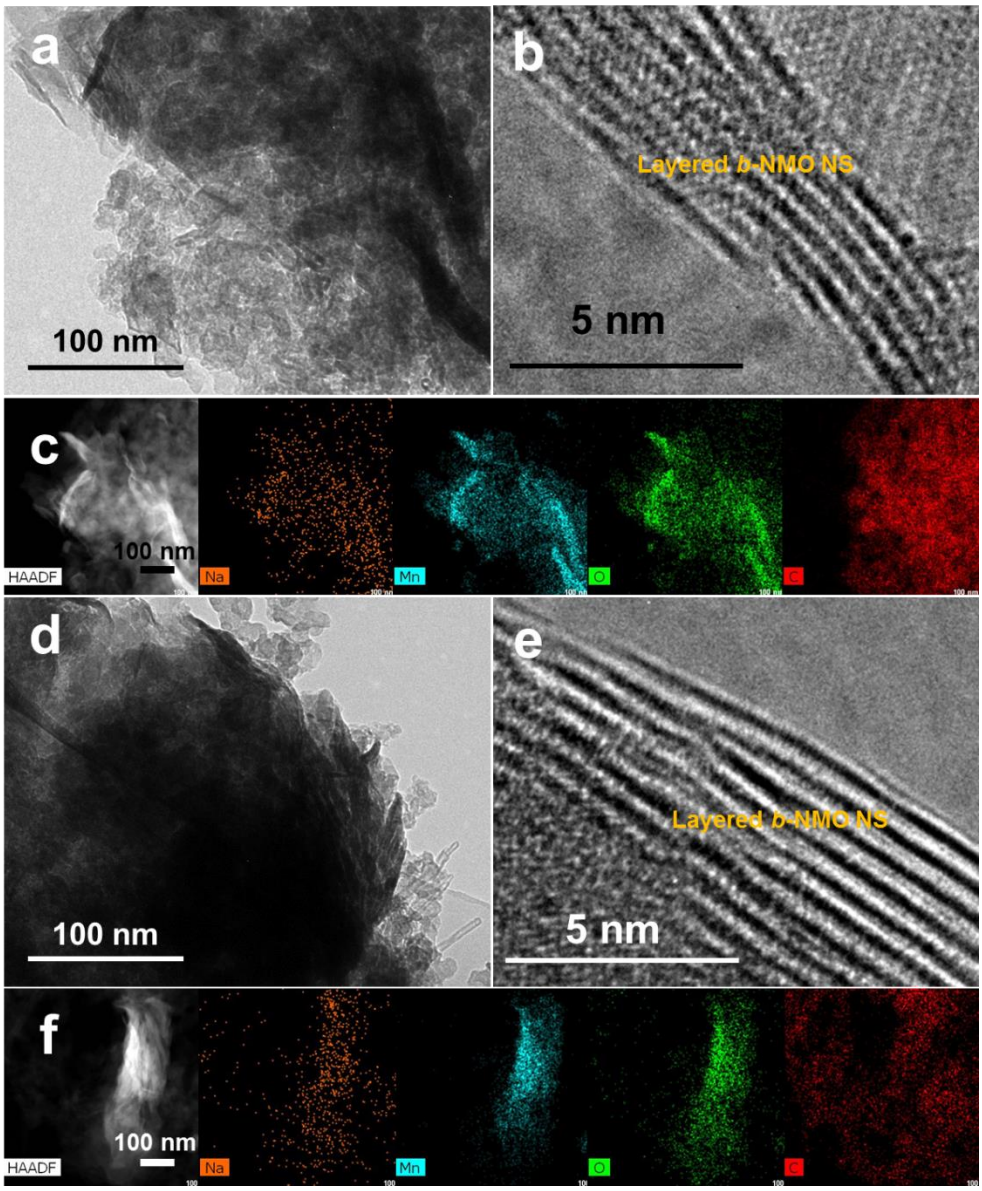

Figure S7. The TEM images, HRTEM images and EDS element mappings of the *b*-NMO/C in the SIBs test collected at various charge/discharge states: charged to 4 V (a-c) and discharged to 1.5 V (d-f), respectively.

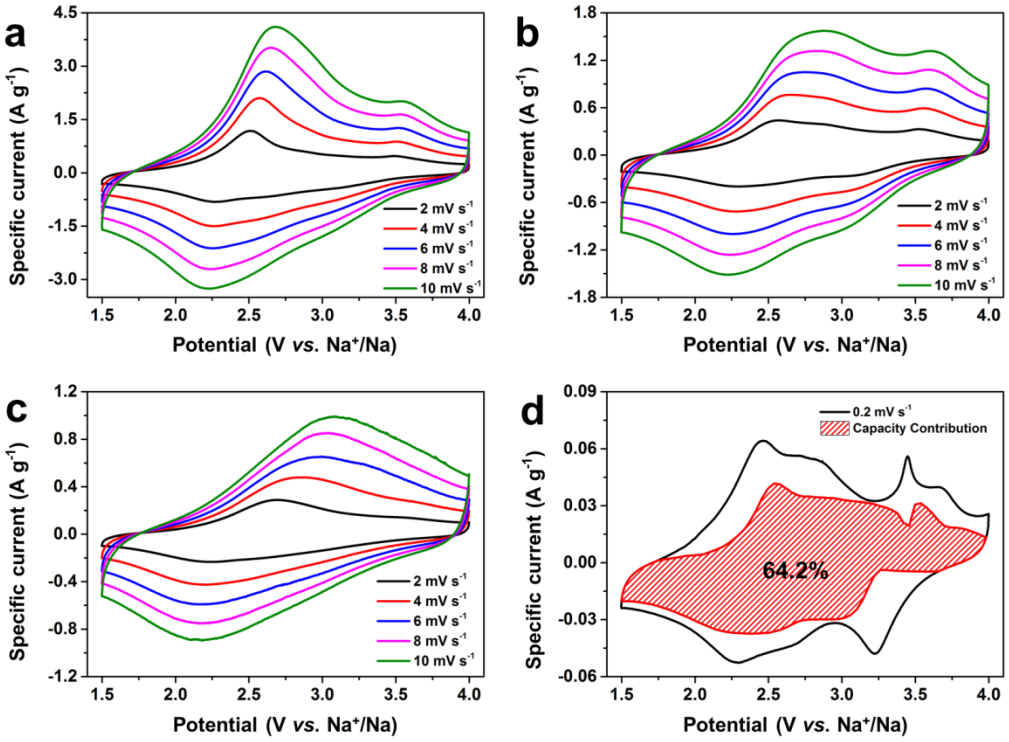

Figure S8. (a-c) CV curves of the *b*-NMO/C, *b*-NMO and *b*-NMO/C-HT at various scan rates from 2 mV s^{-1} to 10 mV s^{-1}. (d) Capacitive contributions (shaded area) to charge storage of the *b*-NMO at a scan rate of 0.2 mV s^{-1}.

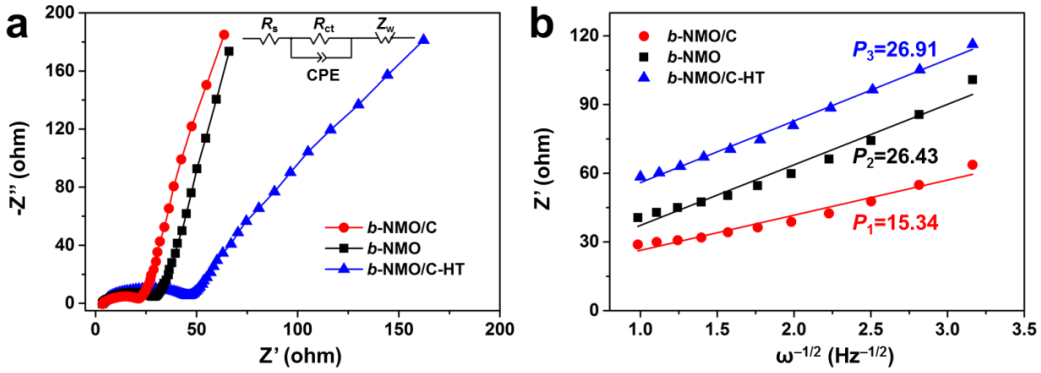

Figure S9. (a) Nyquist plots of the *b*- NMO/C, *b*- NMO and *b*- NMO/C-HT, respectively. (b) Frequency (ω) and Z' values at low frequency region of *b*-NMO/C, *b*-NMO and *b*-NMO/C-HT, respectively.

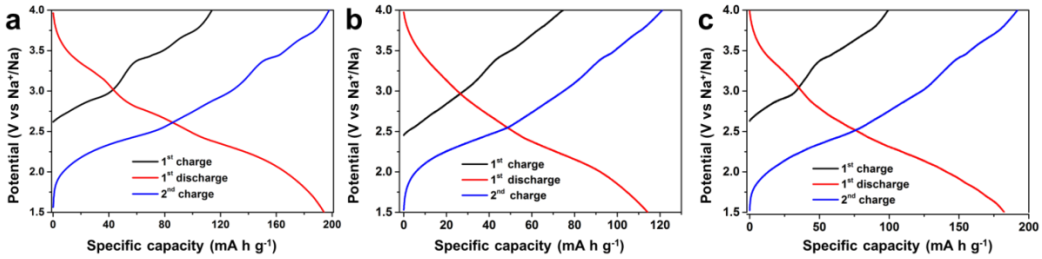

Figure S10. Galvanostatic charge/discharge curves of the *b*-NMO/C (a), *b*-NMO/C-HT (b) and *b*-NMO (c) at 0.25 C, respectively.

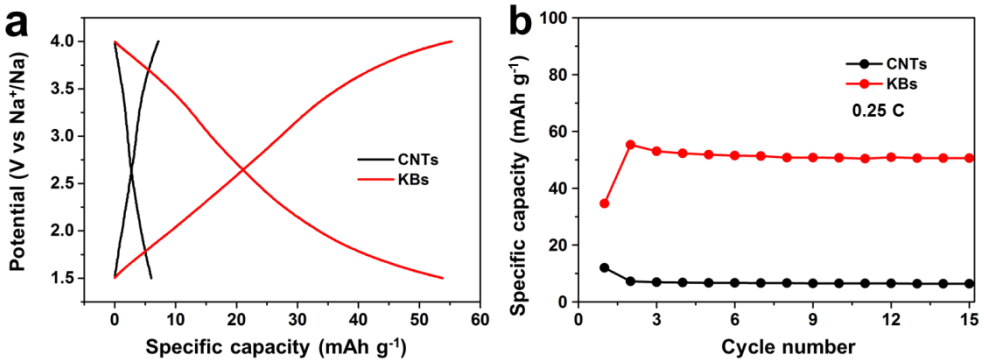

Figure S11. Galvanostatic charge/discharge curves (a) and cycling performances (b) of CNTs and KBs at 0.25 C, respectively.

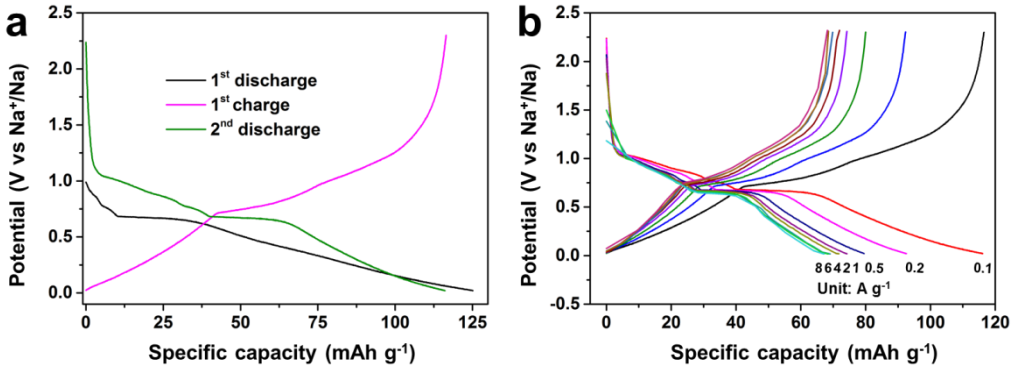

Figure S12. The first two charge/discharge curves (a) and charge/discharge curves at various current densities (b) of graphite.

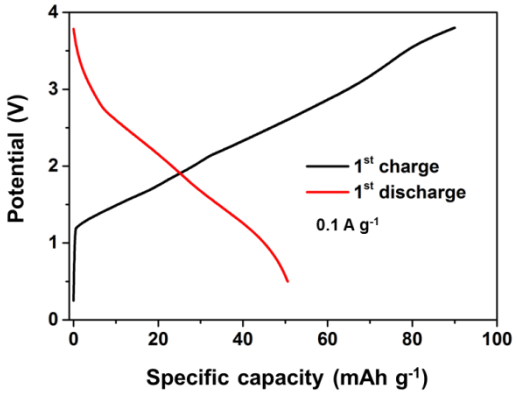

Figure S13. The first charge/discharge curves of the *b*-NMO/C//Graphite SIC.

Table S1. ICP analysis of the *b*-NMO and *b*-NMO/C-HT.

Sample	Na: Mn [at.%]
b-NMO	0.77 : 1
b-NMO/C-HT	0.77 : 1

Table S2. The proportion of different valence of Mn for b-NMO/C according to the XPS analysis.

	Mn^{2+}	Mn^{3+}	Mn^{4+}	Mn valence
Binding energy (eV)	640.1	641.2	642.4	
Area	58030	138000	120485	
percentage	18.75%	38.99%	42.26%	+3.24

Table S3. CHN elemental analysis of the *b*-NMO/C.

Sample	C [wt.%]
b-NMO/C	8.09

Table S4. A comparison for the experimental conditions and cycle capabilities of the state-of-the-art Mn-based SIBs cathodes reported in literatures.

Cathod materials	Ref	Voltage window [V]	The composition of electrode [active material : conductive additives : binder]	Cycling capabilities	Mass loading [mg cm^{-2}]
P2-$Na_{0.8}[Li_{0.12}Ni_{0.22}Mn_{0.66}]O_2$	49	2–4.4	85:10 (acetylene black):5 (PTFE)	50 cycles, 115 mAh g^{-1} (11.8 mA g^{-1})	---
$Na_{0.67}Mn_{0.80}Ni_{0.10}Mg_{0.10}O_2$	50	1.5–4.2	75:15 (super P):10 (PVDF)	50 cycles, 104 mAh g^{-1} (240 mA g^{-1})	---
P2-$Na_{0.45}Ni_{0.22}Co_{0.11}Mn_{0.66}O_2$	51	2.1–4.3	85:10 (super P):5 (PVDF)	100 cycles, 120 mAh g^{-1} (12 mA g^{-1})	2
P2-$Na_{0.66}Ni_{0.33-x}Zn_xMn_{0.67}O_2$	52	2.2–4.25	80:10 (acetylene black):10 (PVDF)	30 cycles, 118 mAh g^{-1} (12 mA g^{-1})	---
P2-$Na_{0.67}Mn_{0.65}Ni_{0.2}Co_{0.15}O_2$	53	1.5–4.2	75:15 (super P):10 (PVDF)	100 cycles, 105 mAh g^{-1} (120 mA g^{-1})	---
$Na_{0.67}[Mn_{0.65}Ni_{0.15}Co_{0.15}Al_{0.05}]O_2$	54	2–4.4	75:15 (acetylene black):10 (PVDF)	50 cycles, 124 mAh g^{-1} (20 mA g^{-1})	---
P2-$Na_{0.5}[Ni_{0.23}Fe_{0.13}Mn_{0.63}]O_2$	55	1.5–4.6	75:15 (carbon black):10 (PVDF)	100 cycles, 125 mAh g^{-1} (100 mA g^{-1})	3
birnessite $Na_{0.77}MnO_2 \cdot 0.5H_2O$	This work	1.5–4	85:10(KBs):5 (PVDF)	100 cycles, 82.8 mAh g^{-1}; 1000 cycles, 51.2 mAh g^{-1} (5000 mA g^{-1})	1-1.5

References

30 K. W. Nam, S. Kim, E. Yang, Y. Jung, E. Levi, D. Aurbach and J. W. Choi, *Chem. Mater.*, 2015, **27**, 150514111747006.

31 W. A. Ang, N. Gupta, R. Prasanth and S. Madhavi, *ACS Appl. Mater. Interfaces*, 2012, **4**, 7011.

32 G. Wang, L. Yi, R. Yu, X. Wang, Y. Wang, Z. Liu, B. Wu, M. Liu, X. Zhang and X. Yang, *ACS Appl. Mater. Interfaces*, 2017, **9**, 25358.

49 J. Xu, D. H. Lee, R. J. Clément, X. Yu, M. Leskes, A. J. Pell, G. Pintacuda, X. Q. Yang, C. P. Grey and Y. S. Meng, *Chem. Mater.*, 2014, **26**, 1260.

50 Z. Li, R. Gao, J. Zhang, X. Zhang, Z. Hu and X. Liu, *J. Mater. Chem. A*, 2016, **4**, 3453-3461.

51 D. Buchholz, A. Moretti, R. Kloepsch, S. Nowak, V. Siozios, M. Winter and S. Passerini, *Cheminform*, 2013, **44**,142-148.
52 X. Wu, J. Guo, D. Wang, G. Zhong, M. J. Mcdonald and Y. Yang, *J. Power Sources*, 2015, **281**, 18-26.
53 Z. Y. Li, R. Gao, L. Sun, Z. Hu and X. Liu, *J. Mater. Chem. A*, 2015, **3**, 16272-16278.
54 D. Yuan, W. He, F. Pei, F. Wu, Y. Wu, J. Qian, Y. Cao, X. Ai and H. Yang, *J. Mater. Chem. A*, 2013, **1**, 3895-3899.
55 I. Hasa, D. Buchholz, S. Passerini, B. Scrosati and J. Hassoun, *Adv. Energy Mater.*, 2015, **4**, 1400083.